Wavelength Dependent Photofragmentation Patterns of Tris(2,2,6,6-tetramethyl-3,5-heptanedionato)Ln (III) (Ln = Eu, Tb, Gd) in a Molecular Beam

ARTICLE *in* THE JOURNAL OF PHYSICAL CHEMISTRY A · JULY 2006

Impact Factor: 2.69 · DOI: 10.1021/jp061763x · Source: PubMed

4 AUTHORS, INCLUDING:

Berry Mary
University of South Dakota
61 PUBLICATIONS **1,195** CITATIONS
SEE PROFILE

Stanley May
University of South Dakota
81 PUBLICATIONS **1,224** CITATIONS
SEE PROFILE

Jeffrey I Zink
University of California, Los Angeles
470 PUBLICATIONS **22,143** CITATIONS
SEE PROFILE

THE JOURNAL OF PHYSICAL CHEMISTRY A LETTERS

2006, *110,* 7751−7754
Published on Web 06/03/2006

Wavelength Dependent Photofragmentation Patterns of Tris(2,2,6,6-tetramethyl-3,5-heptanedionato)Ln (III) (Ln = Eu, Tb, Gd) in a Molecular Beam

Franklin P. Ow,[†] Mary T. Berry,*[,‡] P. Stanley May,[‡] and Jeffrey I. Zink*[,†]

Department of Chemistry and Biochemistry, University of California, Los Angeles, California 90095, and Department of Chemistry, University of South Dakota, Vermillion, South Dakota 57069

Received: March 21, 2006; In Final Form: May 12, 2006

Laser photoionization and ligand photodissociation in $Ln(thd)_3$ (Ln = Eu, Tb, Gd; thd = 2,2,6,6-tetramethyl-3,5-heptanedionato) are studied in a molecular beam via time-of-flight mass spectrometry. The fragmentation patterns are strongly wavelength dependent. With 355 nm excitation, the mass spectrum is dominated by Ln^{2+}, Ln^+, and LnO^+ fragments. The bare Ln ions are believed to arise from photoionization of neutral Ln atoms. The Ln atoms, in turn, are produced from the $Ln(thd)_3$ complex in a sequence of Ln reductions (through ligand-to-metal charge-transfer transitions), with each reduction being accompanied by the dissociation of a neutral ligand radical. In contrast, under visible-light (410−450 nm) excitation, a significant $Ln(thd)_n^+$ signal is observed (where n = 2,3 for Ln = Tb,Gd and n = 1−3 for Ln = Eu). Thus, with visible excitation, photoionization of $Ln(thd)_n$ competes effectively with the Ln-reduction/ligand-dissociation sequence that leads to the dominant bare Ln-ion signal seen with 355 nm excitation. The fact that monoligated $Ln(thd)^+$ is observed only for Ln = Eu is interpreted in terms of the relative accessibility of an excited ligand-to-metal charge-transfer state from the ground electronic state of neutral Ln(thd).

The gas-phase photofragmentation of metal-containing compounds is of interest because of its importance in understanding laser-assisted chemical vapor deposition.[1−5] Only a few photochemical studies of lanthanide-based precursors in the gas phase have been reported,[6−14] in contrast to substantial work on transition-metal complexes.[15−22]

In a study of photoionization mass spectrometry of $Eu(thd)_3$ in a molecular beam, 266 nm nanosecond pulsed-laser excitation produced a mass spectrum dominated by bare europium ions and ligand fragments.[14] A mechanism for metal-ion formation was proposed whereby the excitation light induces a ligand-to-metal charge-transfer (LMCT) transition that results in reduction of the europium ion and creation of a neutral thd radical that rapidly dissociates from the complex. Three sequential metal-reduction/ligand-dissociation steps result in Eu^0 atoms and neutral thd radicals. The ion signal is then generated by subsequent photoionization of these low-mass neutral products.

The experimental observations described above for $Eu(thd)_3$ are similar to those reported for the nanosecond pulsed-laser photoionization of $Co(acetylacetonate)_3$, where Co^+ was the only metal-containing fragment detected.[23] Indeed, metal−ligand bonds are generally weak[24] and a common gas-phase photoionization mechanism involves metal−ligand dissociation followed by ionization.[25−30] The metal ion is usually the largest peak in the mass spectrum, and observation of the parent ion is rare.[31,32]

This communication reports the surprising formation of high-mass metal−ligand complex ions, detected via time-of-flight (TOF) mass spectrometry, under visible-light excitation of $Ln(thd)_3$ (Ln = Eu, Gd, Tb) in a molecular beam. The results of the current study support the photochemical mechanism for the production of bare europium ions proposed[14] and suggest a more complete model for understanding the interplay between the competing photochemical processes that determine whether a high-mass or a low-mass fragmentation pattern is observed.

The UV photoionization TOF mass spectrum of $Eu(thd)_3$ obtained under pulsed (6 ns, 75 mJ/pulse) 355 nm laser excitation is shown in Figure 1 (top). The fragmentation pattern is similar to that reported for 266 nm excitation,[14] with the main difference being the relatively larger EuO^+ signal seen here. In the top panel of Figure 1, the dominant peaks are at 151 and 153 *m*/*z*, corresponding to the two naturally occurring isotopes of Eu^+. At 167 and 169 *m*/*z* are peaks arising from diatomic EuO^+. Another metal-containing species, EuC_2^+, is found at 175 and 177 *m*/*z*. A doublet at 75.5 and 76.5 *m*/*z*, is assigned to Eu^{2+}. The low-mass region exhibits peaks resulting from extensive photofragmentation of the β-diketonate ligand, with *tert*-butyl$^+$ dominating. Mass spectra were obtained at 355 nm with laser-pulse energies ranging from 20 to 75 mJ/pulse (10^8−10^9 W/cm^2). As the fluence decreased, the relative intensities of the ligand fragments and Eu^{2+} decreased, leaving only Eu^+ and EuO^+ observable above the baseline. At the lowest laser

* To whom correspondence should be addressed. E-mail: mberry@usd.edu (M.T.B.); zink@chem.ucla.edu (J.I.Z.). Phone: 605-677-5487 (M.T.B.); 310-825-8651 (J.I.Z.). Fax: 605-677-6397 (M.T.B.); 310-206-4038 (J.I.Z.).
† University of California, Los Angeles.
‡ University of South Dakota.

10.1021/jp061763x CCC: $33.50

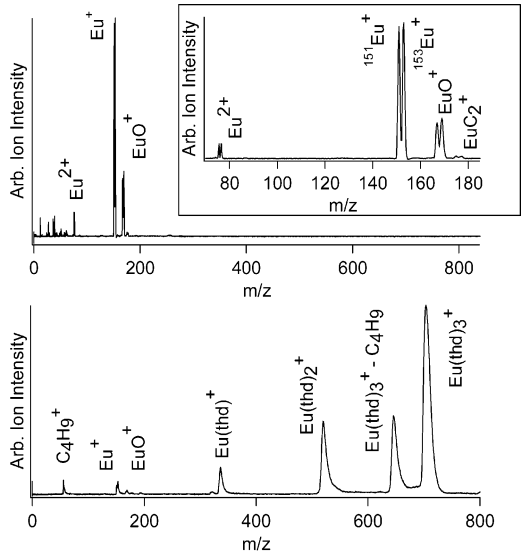

Figure 1. Photoionization mass spectra of $Eu(thd)_3$ under 355 nm (top) and 430 nm (bottom) excitation. The ultraviolet excitation is achieved with the third harmonic of a Nd:YAG laser (75 mJ/pulse) and the visible excitation with a Nd:YAG-pumped OPO (20 mJ/pulse) filtered (KV-389) to remove residual 355 nm light. The dominant peaks with UV light are Eu^{2+}, Eu^+, and EuO^+. With visible light, the parent ion and other ligand-containing fragments are dominant.

fluence, the parent ion was also detected, but with a signal strength less than 1% that of Eu^+.

To determine if the fragmentation pattern is wavelength dependent, TOF mass spectra were measured using visible excitation from a Nd:YAG-pumped optical parametric oscillator (OPO). In the excitation-wavelength region of 410−680 nm, 430 nm excitation resulted in the strongest parent-ion signal, whereas, at wavelengths longer than approximately 470 nm, the parent ion was no longer observable. The shape of this broad and relatively featureless profile results from both variation in ionization cross section and variation in laser power (maximum at ∼450 nm), and we leave its detailed analysis for future work. It does, however, suggest 430 nm as the optimal wavelength for observing the parent ion. The lower spectrum in Figure 1 shows the mass spectrum obtained using 430 nm excitation (20 mJ/pulse), focused for a fluence of $\sim 10^8$ W/cm^2. The mass spectrum obtained from visible-light excitation is dramatically different from that obtained under 355 nm UV excitation (upper spectrum in Figure 1). Surprisingly, at 430 nm, the most intense peaks occur at very high masses, 336, 519, 645, and 702 *m*/*z*. Those features are assigned as $Eu(thd)^+$, $Eu(thd)_2^+$, $[Eu(thd)_3^+-$*tert*-butyl], and $Eu(thd)_3^+$, respectively. $[Eu(thd)_3^+-$*tert*-butyl] represents the parent ion following the loss of a *tert*-butyl group from one ligand. Eu^+, EuO^+, and *tert*-butyl$^+$ are still observed but are minor features in the mass spectrum. These results are unusual, since the parent ion is rarely observed in the photofragmentation spectra of metal-organic compounds obtained with nanosecond pulsed excitation. Fragmentation of weak metal−ligand bonds usually precedes ionization. As mentioned previously, the same high-mass features are weakly observed with 355 nm excitation at the lowest fluences studied (∼20 mJ/pulse), but the bare metal and metal oxide fragments strongly dominate. Our studies clearly show an unusual wavelength selectivity associated with the photochemical behavior of gaseous $Eu(thd)_3$.

To determine if the observation of $Ln(thd)_n^+$ ions using visible-light excitation is unique to Ln = Eu in the $Ln(thd)_3$ series, TOF mass spectra of $Gd(thd)_3$ and $Tb(thd)_3$ were also obtained. The $Tb(thd)_3$ and $Gd(thd)_3$ mass spectra produced by

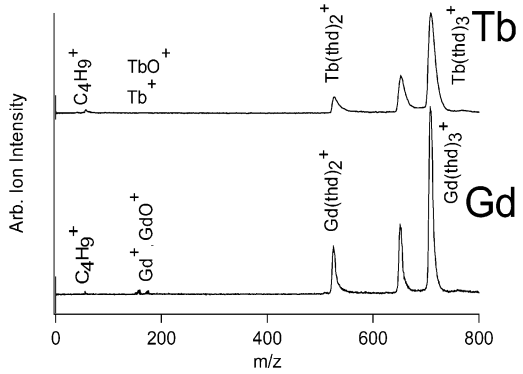

Figure 2. TOF mass spectra of $Tb(thd)_3$ and $Gd(thd)_3$ taken at 430 nm. The parent ion is dominant in both cases. In neither case is $Ln(thd)^+$ evident.

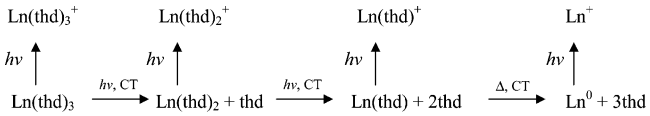

Figure 3. Schematic of $Ln(thd)_3$ photofragmentation and photoionization. The horizontal arrows represent the sequential stripping of neutral ligands from the metal as a result of photon access of ligand-to-metal charge-transfer (LMCT = CT) states. It is suggested that the third ligand may be stripped from Ln(thd) in a zero-photon process using thermal energy residual from the previous steps. Vertical arrows represent photoionization of neutral molecules or bare metal. Single arrows are used to represent multiphoton processes of unspecified order. For example, to the extreme left of the figure, photoionization of $Ln(thd)_3$, yielding the parent ion, $Ln(thd)_3^+$, is represented by a single vertical arrow and requires at least three photons.

355 nm excitation (not shown) are consistent with that of $Eu(thd)_3$, with the dominant peaks being Ln^{2+}, Ln^+, and LnO^+. Figure 2 shows the photoionization mass spectra of $Tb(thd)_3$ and $Gd(thd)_3$ generated using 430 nm excitation. The dominant peaks are $Ln(thd)_3^+$, $[Ln(thd)_3^+-$*tert*-butyl], and $Ln(thd)_2^+$. The peak corresponding to $Ln(thd)^+$ is observed only for europium.

Figure 3 illustrates our proposed reaction model for describing the possible fragmentation outcomes observed in our photoionization spectra. The reaction path moving from left to right along the bottom of Figure 3 represents the sequential metal-reduction/ligand-dissociation steps, which result in Ln^0 atoms and neutral thd radicals. In these steps, absorbance into the charge-transfer state has optimal Franck−Condon overlap at a significantly compressed Eu−O bond length, well above the dissociation limit of the neutral ligand from the complex. Excited at the appropriate wavelength, the neutral ligand will dissociate from the complex in essentially one-half vibrational period. If this lower path dominates, no ions are formed until all ligands are stripped from the lanthanide, such that no high-mass $Ln(thd)_n^+$ (n = 1−3) ions are produced. The vertical arrows in Figure 3 represent competing "side reactions" along each step of the ligand-dissociation pathway, whereby the neutral $Ln(thd)_n$ complexes are directly photoionized to $Ln(thd)_n^+$, resulting in high-mass ions in the spectrum. Thus, the relative rates of the $Ln(thd)_n \rightarrow Ln(thd)_n^+$ direct-ionization reactions and the $Ln(thd)_n \rightarrow Ln(thd)_{n-1}$ + thd ligand-dissociation reactions determine whether a high- or low-mass fragmentation pattern is observed.

Figure 4 shows a single-configurational-coordinate schematic representation for the alternatives of direct multiphoton ionization of $Eu(thd)_3$ to $Eu(thd)_3^+$ versus dissociation of the neutral molecule into the neutral fragments $Eu(thd)_2$ and thd. The lower limit on the ionization continuum, the ionization potential, is estimated from the appearance potential for the parent ion in

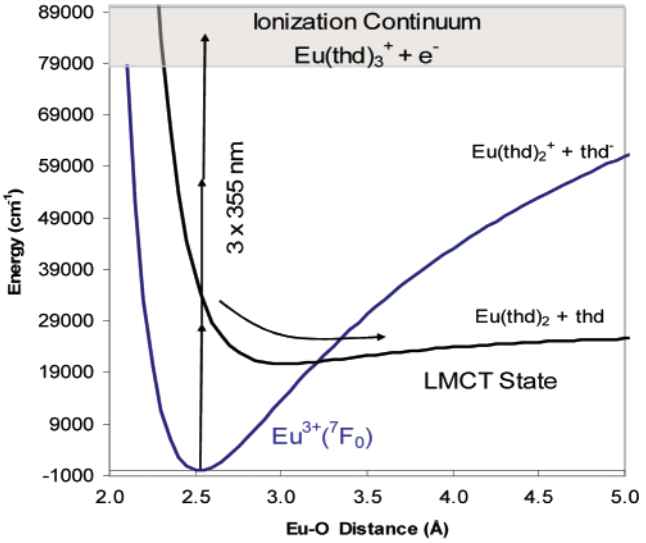

Figure 4. Potential energy diagram for $Eu(thd)_3$, showing multiphoton ionization of the intact molecule in competition with dissociation through the LMCT state into the neutral fragments $Eu(thd)_2$ and thd.

the electron impact mass spectrum.[33] The potential energy curves, which are intended as qualitative representations, rather than rigorously quantitative, are calculated as described in ref 14. Our results suggest that, at 355 nm, dissociation through the charge-transfer state is more efficient than multiphoton ionization of the intact molecule, whereas, at 430 nm, the photoionization process competes quite effectively.

An alternative explanation for the high-mass fragmentation pattern is that all of the $Ln(thd)_n^+$ fragments result from subsequent fragmentation of the parent ion and indeed the same high-mass fragments are observed with electron impact ionization[33] where such a process might be presumed. This mechanism likely accounts for the fact that the parent ion is only observed in the lowest fluence 355 nm experiments and it may still be operative at low fluence for both 355 and 430 nm. However, fragmentation of the parent ion alone does not account well for the observed formation of bare metal ions which are reduced relative to the original Ln(III).

The model shown in Figure 3, invoking photodissociation into neutral fragments, can also be used to account for the primary difference in the high-mass fragmentation patterns for the three $Ln(thd)_3$ complexes, namely, that $Ln(thd)^+$ is detected only for the Eu complex. The activation energy for the formation of Ln^0 + thd from Ln(thd) can be approximated as the crossing point of the potential energy curves of the Ln(thd) electronic ground state and the LMCT state.[14] This step, in contrast to the two previous ligand-dissociation steps, is predicted to occur in a zero- or one-photon process with a moderate thermal barrier. The calculated electrostatic potential energy curves (as a function of lanthanide−oxygen bond distance) for the ground state and lowest LMCT state of Ln(thd) yield an estimated crossing point for Eu(thd) which is greater than that for Tb(thd) which is, in turn, greater than that for Gd(thd). The difference in barrier heights results from differences in the first ionization energies, IP_1. For example, IP_1 is lowest for Eu, therefore lowering the Eu(I) ground state relative to the Eu(0) LMCT state and effectively raising the barrier to LMCT access. The implication, therefore, is that only for Eu(thd) is the ligand-dissociation barrier high enough to permit competition from direct Eu(thd) → $Eu(thd)^+$ photoionization. To test this model, the photoionization mass spectrum of $Pr(thd)_3$ was measured. Praseodymium exhibits a first ionization potential lower than that of europium

TABLE 1: Slope, *n*, of log(*I*) versus log(P/P_0) Power Plots[a]

ion species	$Eu(thd)_3$	$Gd(thd)_3$	$Tb(thd)_3$	AP[33]
$Ln(thd)_3^+$	2.4 ± 0.2	2.6± 0.1	2.5± 0.4	3.4
$Ln(thd)_3^+$−*tert*-butyl	3.1 ± 0.1	3.7 ± 0.1	2.9 ± 0.2	4.4
$Ln(thd)_2^+$	4.0 ± 0.1	4.0 ± 0.3	4.2 ± 0.4	5.8
$Ln(thd)^+$	6.0 ± 0.4			8.3

[a] Laser-pulse energies range from 7 to 20 mJ/pulse, focused for a fluence of ~10^8 W/cm^2. Errors are for the 95% confidence limits on the fitted slopes. Also given are the 430 nm photon number equivalents of the reported appearance potentials (APs) for $Eu(thd)_3$.[33] For $Ln(thd)_3^+$, the power plots show evidence of saturation at the higher powers. The slope at low power approaches 3, and this is thought to be the most likely photon dependence.

which results in a higher barrier to neutral dissociation of Pr(thd). At 430 nm and 10^8 W/cm^2, the photoionization mass spectrum of $Pr(thd)_3$, unlike $Tb(thd)_3$ and $Gd(thd)_3$, exhibits a prominent $Ln(thd)^+$ feature. It is worth noting that the $Pr(thd)^+$ feature does not appear in the electron impact mass spectrum of ref 33.

To explore the number of photons involved in the formation of the high-mass ions, power studies were conducted with 430 nm excitation. The logarithm of the ion-signal intensity, log(*I*), for each of the species was plotted versus the logarithm of the relative laser power, log(P/P_0), yielding linear plots with slopes, *n*. The slopes provide a lower limit for the number of photons required for ion formation.

For the formation of $Eu(thd)_3^+$, $Gd(thd)_3^+$, and $Tb(thd)_3^+$, power-dependence measurements yielded slopes of $n = 2.4$, 2.6, and 2.5, respectively. Saturation effects are evident in the curvature of several of the plots at the highest laser powers. For example, the slope for $Eu(thd)_3^+$ gradually increases from 2.4 to ~3 as the high-energy points, most subject to saturation effects, are sequentially eliminated. The most logical inference from these results is that production of each of the three $Ln(thd)_3^+$ ions has a minimum photon dependence of 3. The similar power dependence seen for each parent ion can be understood in terms of ionization occurring via removal of an electron from a ligand; the ligand, therefore, becomes a resonance-stabilized radical, and the Ln(III) remains in its original oxidation state. This interpretation is consistent with the observation of the [$Ln(thd)_3^+$−*tert*-butyl] fragment in the mass spectrum, because the ligand radical, still bound in the parent ion, can easily rearrange to eliminate a *tert*-butyl radical:

$$[(CH_3)_3C{-}CO]_2CH\bullet \rightarrow (CH_3)_3C{-}CO{-}CH{=}C{=}O + (CH_3)_3C\bullet$$

According to our model in Figure 3, $Ln(thd)_2^+$ production first requires the formation of neutral $Ln(thd)_2$ (following laser excitation to a LMCT state of $Ln(thd)_3$) and subsequent photoionization of $Ln(thd)_2$. The data in Table 1 suggest that this requires four or more photons and that the analogous process for $Eu(thd)^+$ requires six or more.

Table 1 also shows a comparison of our power-dependence results with the electron impact appearance potentials (APs) reported for $Eu(thd)_n^+$.[33] The AP gives an upper limit on the ionization potential. For ease of comparison, the AP units have been converted to the equivalent number of 430 nm photons.

Visible-light laser-photoionization mass spectrometry of $Ln(thd)_3$ provides an unprecedented opportunity to visualize the mechanism whereby bare metal ions and atoms are produced in the photofragmentation of gas-phase metal−organic complexes. In the mass spectrum, snapshots of each of the neutral intermediates are provided by photoionization of those inter-

mediates, competing effectively with the neutral dissociation steps which proceed to Ln^0. In future work, we will examine wavelength control for strategies that either optimize this mechanism for ligand stripping, yielding the bare metal product, or, alternatively, reduce the efficiency of this path and optimize other competing routes which result in the production of metal oxides (observed but not discussed in this work), or with a different ligand, production of metal nitrides for chemical vapor deposition.

Acknowledgment. This work was made possible by a grant from the National Science Foundation to J.I.Z. (CHE-0507929). Acknowledgment is made to the Donors of the American Chemical Society Petroleum Research Fund for partial support of this research (M.T.B. and P.S.M.).

Supporting Information Available: The experimental design for the TOF mass spectrometer and laser setup is described in detail. Power law plots from which the data in Table 1 are extracted are also given. This material is available free of charge via the Internet at http://pubs.acs.org.

References and Notes

(1) Morosanu, C. E. *Thin Films by Chemical Vapor Deposition*; Elsevier: New York, 1990.

(2) Eden, J. G. *Photochemical Vapor Deposition*; Wiley: New York, 1992.

(3) Hitchman, M. L.; Jensen, K. F. *Chemical Vapor Deposition*: *Principles and Applications*; Academic Press: San Diego, CA, 1993.

(4) Kodas, T. T.; Hampden-Smith, M. J. *The Chemistry of Metal CVD*; Weinheim: New York, 1994.

(5) Braichotte, D.; Garrido, C.; van den Bergh, H. *Appl. Surf. Sci.* **1990**, *46*, 9−18.

(6) Paeivaesaari, J.; Putkonen, M.; Niinistoe, L. *Thin Solid Films* **2005**, *472*, 275−281.

(7) Santos, L. S.; Petrucelli, G. P.; Airoldi, C. *Polyhedron* **1999**, *18*, 969−977.

(8) Hosoya, N.; Takegami, R.; Suzumura, J.; Yada, K.; Koyasu, K.; Miyajima, K.; Mitsui, M.; Knickelbein, M. B.; Yabushita, S.; Nakajima, A. *J. Phys. Chem. A* **2005**, *109*, 9−12.

(9) Corpillo, D.; Cabella, C.; Crich, S. G.; Barge, A.; Aime, S. *Anal. Chem.* **2004**, *76*, 6012−6016.

(10) Bassett, A. P.; Magennis, S. W.; Glover, P. B.; Lewis, D. J.; Spencer, N.; Parsons, S.; Williams, R. M.; De Cola, L.; Pikramenou, Z. *J. Am. Chem. Soc.* **2004**, *126*, 9413−9424.

(11) Kurikawa, T.; Negishi, Y.; Hayakawa, F.; Nagao, S.; Miyajima, K.; Nakajima, A.; Kaya, K. *Eur. Phys. J. D* **1999**, *9*, 283−287.

(12) Gibson, J. K. *Anal. Chem.* **1997**, *69*, 111−117.

(13) (a) Campbell, M. L. *J. Chem. Phys.* 1999, *111*, 562. (b) Campbell, M. L. *J. Phys. Chem. A* **1999**, *103*, 7274. (c) Campbell, M. L. *Phys. Chem. Chem. Phys.* **1999**, *1*, 3731−3735.

(14) Nelson, B. N.; Caster, A. G.; Berry, M. T. *Chem. Phys. Lett.* **2004**, *396*, 256−260.

(15) Lou, X.; van Buijtenen, J.; Bastiaansen, J. J. A. M.; de Waal, B. F. *J. Mass Spectrom.* **2005**, *40*, 654−660.

(16) Gruhn, N. E.; Michelsen, L. J.; Westcott, B. L. *Inorg. Chem.* **2002**, *41*, 5907−5911.

(17) Ketkov, S. Y.; Selzle, H. L.; Heinrich, L.; Schlag, E. W. *Isr. J. Chem.* **2004**, *44*, 65−69.

(18) Ketkov, S. Y.; Selzle, H. L.; Heinrich, L.; Schlag, E. W. *Mol. Phys.* **2004**, *102*, 1749−1757.

(19) Ketkov, S. Y.; Selzle, H. L.; Heinrich, L.; Schlag, E. W. *J. Chem. Phys.* **2004**, *121*, 149−156.

(20) Ketkov, S. Y.; Selzle, H. L.; Heinrich, L.; Schlag, E. W.; Titova, S. N. *Chem. Phys.* **2003**, *293*, 91−97.

(21) Ketkov, S. Y.; Selzle, H. L.; Heinrich, L.; Schlag, E. W.; Domrachev, G. A. *Chem. Phys. Lett.* **2003**, *373*, 486−491.

(22) Ketkov, S. Y.; Selzle, H. L.; Heinrich, L.; Schlag, E. W.; Domrachev, G. A. *Inorg. Chem. Commun.* **2002**, *5*, 909−912.

(23) Grun, C.; Heinicke, R.; Weickhardt, C.; Grotemeyer, J. *Int. J. Mass Spectrom.* **1999**, *185*−*187*, 307−318.

(24) (a) Sharp, P.; Richardson, D. E. *J. Am. Chem. Soc.* **1991**, *113*, 8339. (b) Giera, E. *J. Chem. Thermodyn.* **2000**, *32*, 821−833.

(25) Muraoka, P.; Byun, D.; Zink, J. I. *J. Am. Chem. Soc.* **2000**, *122*, 1227−1228.

(26) Cheon, J.; Muraoka, P.; Zink, J. I. *Chem. Mater.* **2000**, *12*, 511−516.

(27) Bitner, T. W.; Zink, J. I. *Inorg. Chem.* **2002**, *41*, 967−972.

(28) Muraoka, P.; Byun, D.; Zink, J. I. *Coord. Chem. Rev.* **2000**, *208*, 193-211.

(29) Gedanken, A.; Robin, M. B.; Kuebler, N. A. *J. Phys. Chem.* **1982**, *86*, 4096−4107.

(30) Schlag, E. W.; Neusser, H. J. *Acc. Chem. Res.* **1983**, *16*, 355−360.

(31) Muraoka, P.; Byun, D.; Zink, J. I. *J. Phys. Chem. A* **2001**, *105*, 8665−8671.

(32) Byun, D.; Zink, J. I. *Inorg. Chem.* **2003**, *42*, 4308−4315.

(33) McDonald, J. D.; Margrave, J. L. *J. Less-Common Met.* **1968**, *14*, 236−239.